

# New developments in material testing at very high strain rates

Grams R.<sup>1</sup>, Fang X.F.<sup>1</sup>

<sup>1</sup> University of Siegen, Institute for Automotive Lightweight Design, Siegen, Germany

## Abstract

The determination of material properties under high-speed loading has been a challenge for many years. Structural vibrations, also called system ringing, in conventional testing machines deteriorate the quality of force measurement, which makes a precise determination of stress-strain curves and corresponding mechanical properties impossible.

In this work, a new specimen geometry with its basic mechanical principle and the corresponding measurement technique are presented and discussed. The new method allows the determination of true stress-strain curves at high strain rates free from oscillation.

Due to the additionally minor plastic deformation area in the new Generation III specimen, a quasi-movable bearing condition for the specimen fixation was created. Forces, based on the natural frequency of the specimen, deform the cross-section and create a displacement, which keeps the kinetic energy of the measurement area high. In this way, the elastic ringing effect has been reduced significantly. Any kind of filtering, smoothing or similar manipulations of the result are no longer needed.

This new method has been validated on three steels types and one type of aluminium alloy with different strain hardening behavior through measurements and numerical analysis. The Generation III specimen can also be used for the quasi-static test and cover the strain rate range from  $4.4 \cdot 10^{-4}$  -  $10^3$  /s accordingly.

**Keywords** specimen geometry · high-speed tensile test · servo-hydraulic testing machine · stress wave analysis · material characterization · stress-strain curve · strain rate · crash simulation

## 1 Introduction and state of the art

In a vehicle crash, large multi-axial deformations can occur with strain rates in the range of  $10^{-4}$  -  $10^3$  /s, which must be correctly mapped by finite element method (FEM) during vehicle development.

In order to determine flow curves in the strain rate range  $4.4 \cdot 10^{-4}$  -  $10^3$  /s, three different measuring techniques are generally used: quasi-static testing machine with long tensile specimen (80 mm gauge length) for  $4.4 \cdot 10^{-4}$  -  $10^2$  /s; servo-hydraulic high-speed testing machine with smaller tensile specimens (20 - 25 mm gauge length) for the range up to  $10^3$  /s; Split-Hopkinson-Bar (SHB) for the range  $> 10^3$  1/s with very small specimens ( $< 10$  mm gauge length). The experimental techniques and conditions, i.e. the measurement of force, deformation, specimen geometry and size as well as the specimen fixation, are different for the strain rate ranges and produce an apparent discontinuity in material behavior [1].

The use of the different experimental techniques is based on one hand on the different maximum pull-off speeds and on the other hand on the force signal oscillations at high strain rates, the so-called system ringing effect [2]. Xiao et al. [2] stated that the insertion of a rubber damper in the force introduction increases the force rise time in such an experiment so that the stress wave has time to move back and forth at least three times within the specimen. This allows a quasi-equilibrium of the force within the specimen to be approximated and the oscillation of the force signals to be reduced. Zhu [3] used the mode analysis of the entire system to filter out the force signal oscillations by using the eigenfrequencies and amplitudes of the system. While the method in [2] also reduces the maximum achievable strain rate and counteracts the goal of the high-speed test, signal filtering is an important intervention in the measurement data. In [4,5] suitable specimen geometries, measuring techniques and filtering were developed and recommended by extensive investigations. With the SEP

1230 [4], a specimen with a measuring length of 20 mm is given the highest possible natural frequency in order to reduce the vibration amplitude. In addition, the force measurement should be carried out as close as possible to the gauge length of the specimen at the specimen shoulder by the use of strain gauges instead of using a load cell [5]. With this method, flow curves with reduced oscillations can be obtained up to approx. 200 /s.

As is well known, a Split Hopkinson Bar (SHB) without oscillation of the force signals can be used for the range  $> 10^3$  /s. However, the results of such experiments by different research groups for one and the same material are considerably different. Verleysen et.al. stated [6] that in a SHB experiment many of the fundamental assumptions for the evaluation of the test results are not valid in reality. The stress and strain in the very small specimens are by no means homogeneous as assumed and the achievement of a quasi-static equilibrium is not always given. This leads, among other things, to an overestimation of the deformations and deviation of the determined stresses.

## 2 Wave propagation and system vibration analysis

Thanks to decades of efforts by the SHB community, the theory of stress waves in solids is well established. This theory was used in [7] to develop and validate a FEM model, whereby the accuracy of the FEM model was confirmed by Zwick both on the basis of simple specimens and on a complex system consisting of steel specimens, specimen grips, load cells, and test system sliding bar.

In [8], a phenomenon was discovered that can be seen in Fig. 1: While the oscillations in the area of the sliding bar are extremely large and very large in the area of the load cell, they are very small in the gauge length of the specimen.

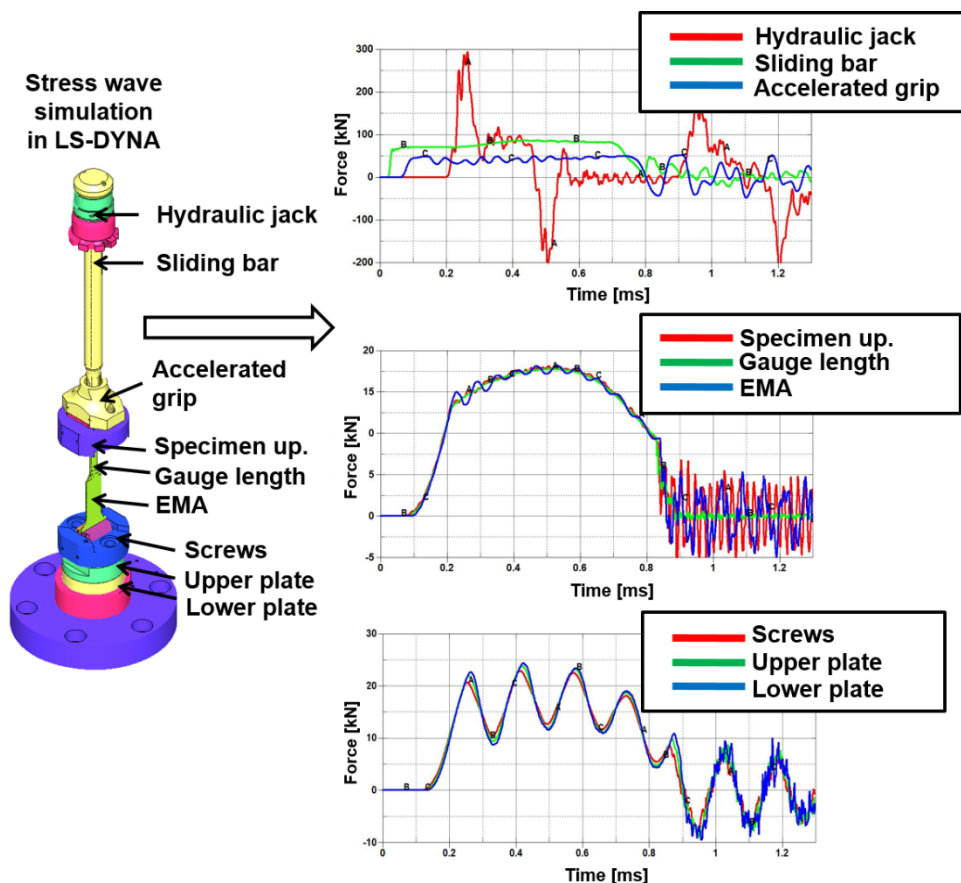


Fig.1: Analysis of force fluctuations at different positions of the test system (EMA: Elastic measurement area)

### 3 Solution approaches and development of the new method

The above conclusion is used as a starting point for the development of a new specimen geometry. Since the force oscillations in the area of the specimen with large plastic deformation are very low, it is assumed that the system oscillations are determined by the boundary conditions of the system. Mechanically, this plastic deformation, which also causes a displacement of the specimen body, can also be interpreted as a change in the bearing conditions of a vibrating rod. The tensile test specimen is presented as a vibrating rod element.

For a conventional tensile test with the known specimens, the following conclusions can be presented. The upper end of the specimen (Fig. 1), which is connected to the so-called sliding bar of the testing machine, is always movable and therefore represents a movable bearing, while the lower end is connected to the load cell and is therefore regarded as a fixed bearing. Further FEM calculations show that the elastic vibrations of the sample are almost zero if the sample is also loosely supported instead of fixed at the lower end. Therefore, in a second shoulder area of the modified SEP sample developed in [7,8], local reduction of the cross-section was introduced (Fig. 2). These weakening should allow a slight and local plastic deformation in the second shoulder area of the specimen and thus a quasi-movable bearing.

Thus, the elastic oscillations in the 2nd shoulder area of the specimen should be significantly reduced in order to measure the force in this area as in [7,8]. The force can then be measured either optically as in [7,8] or locally on the sample via strain gauges.

The conditions for an almost vibration-free force measurement in the second shoulder area of the specimen are now described in detail with the help of Fig. 3. At the same time, it is ensured that the actual major plastic deformation of the specimen in the gauge length remains undisturbed.

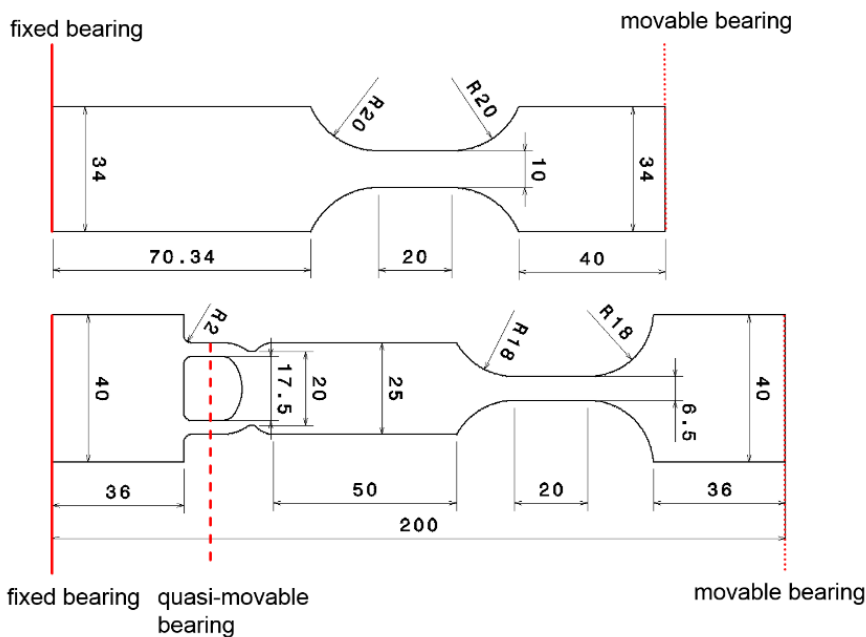


Fig.2: Comparison of different specimen. Upper: SEP 1230; Lower: New Generation III specimen (Gen. III)

The specimen geometry with the best results, the so-called Generation III specimen (Fig. 2 bottom and Fig. 3), has five sections (section 2 - 6) with different widths in addition to the two specimen clamping areas (section 1 and 7). The force in the tensile test is applied in section 1, while the specimen is firmly clamped and immovable in section 7. In section 3, the actual major plastic deformation up to fracture shall take place. Section 5 is dimensioned larger than section 3. In section 5 another section 6 with geometric weaknesses is introduced. The geometrical dimensions of the specimen must fulfill different conditions:

$$\text{Section 3: } \frac{R_{mB3} \cdot A_{B3}}{R_{mB6} \cdot A_{B6}} < 1 \quad (1)$$

$A_{B(n)}$ : Cross-section in section (n) with (n) = 1-7 (Fig.3);  $R_{mB(n)}$ : Tensile strength of the material in section (n)

This ensures that mainly section 3 is deformed. In this section, the specimen deformations are measured to calculate the strains. For a homogeneous quasi-isotropic material,  $R_{p0.2}$  and  $R_m$  are the same in all sections. The following condition must apply in the force measurement area:

$$\text{Section 5: } \frac{R_{mB3} \cdot A_{B3}}{R_{p0.2B5} \cdot A_{B5}} \leq 1 \quad (2)$$

$R_{p0.2B(n)}$ : Yield strength of the material in section (n)

This ensures that only purely elastic deformations occur in section 5. The force is measured locally via strain gauges or via digital image correlation (DIC).

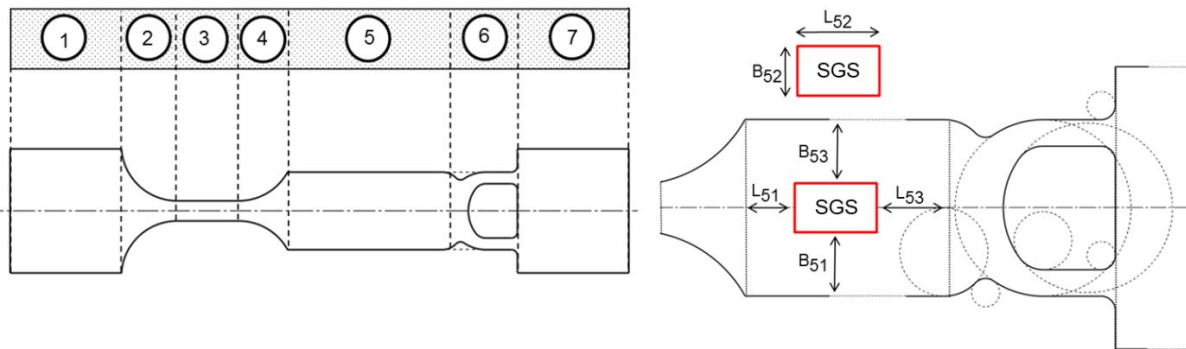


Fig.3: Gen. III specimen geometry and its characteristics (SGS: Strain gauge sensor)

The following conditions must be met in section 6 of the specimen:

$$\text{Section 6: } \frac{R_{p0.2B6}}{R_{mB3}} \leq \frac{A_{B3}}{A_{B6}} < \frac{R_{mB6}}{R_{mB3}} = 1 \quad \text{for homogeneous materials} \quad (3)$$

This is to ensure that section 6 is slightly plastically deformed during the test while section 3 undergoes the major deformations. In this way the bearing conditions for section 5 change from fixed to quasi-movable and oscillation in the force measuring area are avoided as far as possible.

Extensive investigations show that the shape and position of the local weakening in section 6 in coordination with section 5 must be designed accordingly so that a sufficiently large area is created in section 5 in which a homogeneous strain field prevails in order to be able to measure the force accurately and oscillation-free. Therefore, the weakening of the section has both a special inner and outer shape.

The results of the high-speed tests on two steels in the following chapter 4 prove that oscillation-free force measurement up to nominal strain rates of  $\dot{\epsilon} = 1000$  /s has now become possible.

A further problem was taken into account in the evaluation. This is the problem caused by the difference of force and deformation measurement. The deformation measurement is carried out in section 3 of the specimen (as usual). It can be done via strain gauges or DIC (e.g. via GOM ARAMIS). However, the force measurement cannot be carried out in section 3 but only in section 5 (Fig. 3). As shown in Fig. 4 below left, both measuring positions are 48 mm apart.

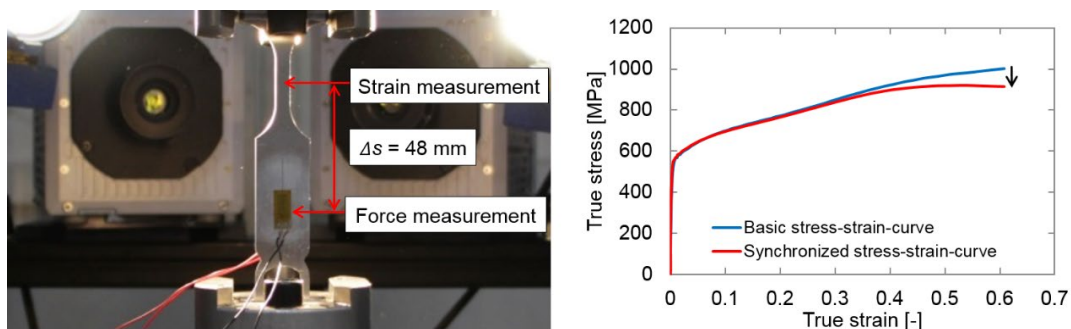


Fig.4: Different measurement positions for force and deformation and their effect

The force and deformation measurements are therefore time-shifted. This time offset can be calculated with the simple equation 4. If the speed of sound in steel is chosen with 5850 m/s, the stress or force, which can be assigned to the deformation measurement in section 3, needs 8.21  $\mu$ s to be measured in section 5 by e.g. strain gauges. If this time delay is neglected, a stress increase of almost 100 MPa occurs on a DP600 specimen as shown in Fig. 4 on the right.

$$\text{Speed of Sound } c: \quad c = \lambda \cdot f \approx \frac{\Delta l}{\Delta t} \quad (4)$$

$\lambda$ : wavelength;  $f$ : frequency;  $\Delta l$ : travel distance;  $\Delta t$ : travel time

#### 4 Results on strain rate dependence

With the above-mentioned method, the strain rate dependencies of the flow curves of steel DC 04 and DP 600 are measured and systematically investigated. A Zwick Z100 testing machine was used for the quasi-static tests. The deformations were measured with a GOM 5M CCD camera (max. frame rate: 29 Hz; max. resolution: 2448 x 2050). The high-speed tests were carried out using a Zwick HTM 5020 testing machine. A PHOTRON SA 5 camera (max. frame rate: 1 MHz; max. resolution 1024 x 1024) was used for the deformation measurement. However, the resolution of the camera had to be limited to 128 x 240 pixels in order to achieve the required high clock frequency of 150 kHz in the high-speed test up to 1000 /s. The measurement data were all post-processed with the GOM ARAMIS software and then evaluated using a proprietary software package.

The following nominal strain rates,  $4.4 \cdot 10^{-4}$  /s, 25 /s, 100 /s, 200 /s, 300 /s, 500 /s, 1000 /s, were realized. The same Gen. III specimen was used for all strain rates so that any specimen geometry effects are excluded. The entire strain rate range from  $4.4 \cdot 10^{-4}$  -  $10^3$  /s could be measured with a single specimen geometry and measurement technique.

The stress-strain curves are shown in Fig. 5(a). Three tests were performed for each strain rate. The fluctuations of the flow curves are small. It should be emphasized that all flow curves are pure measurement data without any filtering.

After these three flow curves are being approximated using a cubic spline function, averaging and differentiation take place, which results in a clear hardening behavior (hardening rate  $d\sigma/d\varepsilon$  versus yield stress plotted) in Fig. 5(b). The hardening rate increases with increasing strain rate. This is particularly pronounced in the area of higher stresses. However, there is an anomaly at 500 /s which could not yet be explained. On the other hand, the unusual flow and hardening curves at 100 /s can be explained by the conditions of the Zwick testing machine (insufficient energy input at lower speed and readjustment of the hydraulic cylinders).

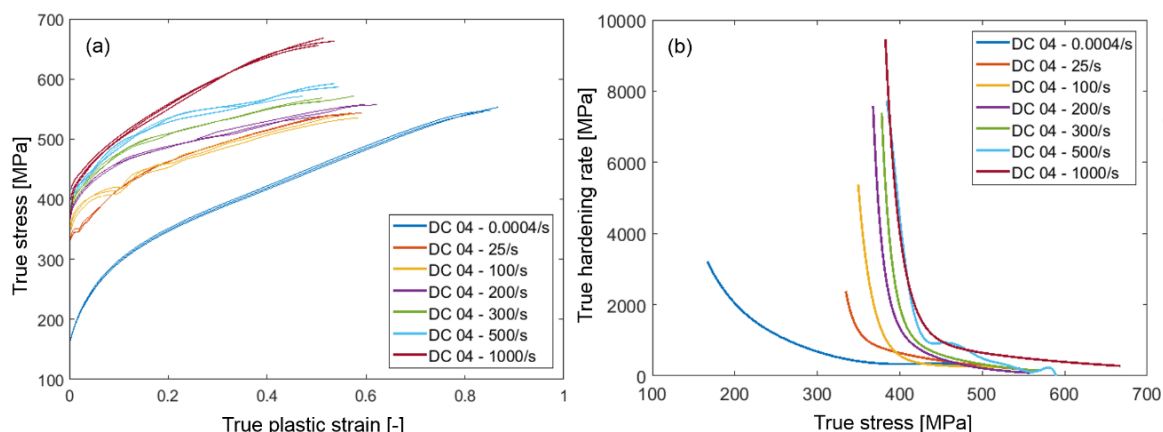


Fig.5: True stress-strain curves of steel DC 04 (a) and the corresponding strain hardening curves (b)

Fig. 6 summarizes the strain rate dependence of the yield strength and the tensile strength of the two steels. It should be noted that the set nominal strain rates have not yet been reached when measuring the yield strength, while these are already exceeded when measuring the tensile strength. Therefore, the yield strengths and the tensile strengths are plotted against the real strain rates. It should be mentioned that the strain rates can increase 6 - 7 times due to the uncontrolled testing machine. This appearance can easily be explained by the increasing localization of the plastic deformation zone at the specimen (necking).

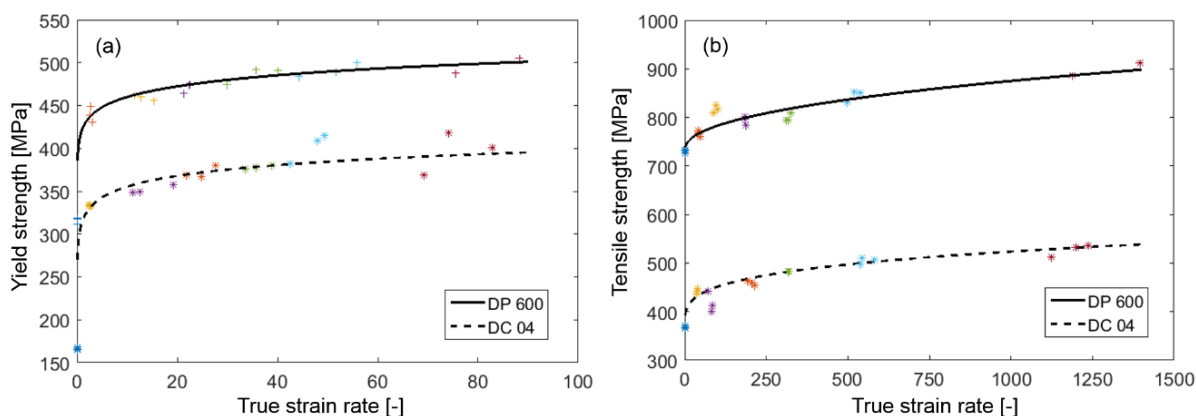


Fig.6: Strain rate dependence of the yield strength (a) and the tensile strength (b) of DC 04 and DP 600

## 5 Summary

A... Through the FEM modeling of the entire servo-hydraulic test system in combination with physical mechanical ideas, a novel specimen geometry with a corresponding measuring method was developed in this work. This allows an oscillation-free force measurement at strain rates of up to 5000 /s to be performed. This method can be used for the entire strain rate range of  $4.4 \cdot 10^{-4}$  -  $10^3$  /s and enables a continuous determination of material properties for crash calculation. Measurements on steel materials confirm the method and showing a clear strain rate dependence.

## 6 Literature

- [1] T.J. Cloetea and M. Stander: Refinement of the wedge bar technique for compression tests at intermediate strain rates, EPJ Web of Conferences 26, 01025 (2012), DYMAT 2012
- [2] X. Xiao: Dynamic tensile testing of plastic materials, Polymer Testing 27 (2008), S. 164-178

- [3] D. Zhu, S. Rajan, B. Mobasher, A. Peled, and M. Mignolet: Modal Analysis of a Servo-Hydraulic High Speed Machine and its Application to Dynamic Tensile Testing at an Intermediate Strain Rate, *Experimental Mechanics* 51(2011), S. 1347-1363
- [4] Ermittlung mechanischer Eigenschaften an Blechwerkstoffen bei hohen Dehnraten im Hochgeschwindigkeitsdehnversuch, SEP 1230, Stahl-Eisen-Prüfblätter (SEP), Feb-2007.
- [5] W. Böhme: FAT-Richtlinie, Dynamische Werkstoffkennwerte für die Crashsimulation, FAT, Frankfurt am Main, 2007
- [6] P. Verleysen: Numerical study of the influence of the specimen geometry on split Hopkinson bar tensile test results, *Latin American Journal of Solids and Structures* 6 (2009), S. 285-298
- [7] J. Li and X.F. Fang: Stress Wave Analysis and Optical Force Measurement of Servo-Hydraulic Machine for High Strain Rate Testing, *Exp Mech.* 54 (2014), S. 1497-1501
- [8] X.F. Fang and J. Li: Numerical stress wave analysis in LS-DYNA and force measurement at strain rates up to 1000 1/s of a high speed tensile machine, in "LS-DYNA Forum", Bamberg, Okt. 2014